# Mesoporous and amorphous Ti–silicas on the epoxidation of vegetable oils

L.A. Rios, P. Weckes, H. Schuster, W.F. Hoelderich [*]

*Department of Chemical Technology and Heterogeneous Catalysis, RWTH Aachen University, Worringerweg 1, 52074 Aachen, Germany*

## Abstract

For the epoxidation oleic acid methyl ester, different kinds of Ti–MCM-41 materials and Ti–amorphous silicas were compared. Catalytic activity was explained in terms of chemical and textural features of the denoted materials. Further examinations were made of the behavior of reaction temperature and different solvents, Ti-loading of the catalysts, and their re-usability and stability. Mesoporous materials like MCM-41 used as a Ti-support have the advantage of its higher surface area toward amorphous Ti–SiO$_2$. The structure of Ti–MCM-41 was not observed to play any important role in the activity. Ti–SiO$_2$ proved to be a truly heterogeneous catalyst and could be reused at least four times. The epoxidation system TBHP/Ti–SiO$_2$ has not been reported so far in the literature for the epoxidation of vegetable oils and their transesterification products. Based on the results presented here, this system could have a great potential for industrial use.
© 2005 Published by Elsevier Inc.

*Keywords:* Oils; Epoxidation; Ti–MCM-41; Ti–silica

## 1. Introduction

Epoxidation of plant oils, commonly referred to as "vegetable oils," is a commercially important reaction because the epoxides obtained from these renewable raw materials and from the methyl oleate, their transesterification product, have applications in such materials as plasticizers and polymer stabilizers [1,2]. The mass and dimension of the methyl oleate are about one-third of those of the triglyceride, the main component of vegetable oils. Furthermore, these epoxides (the epoxidized oleates) can be used as intermediates in the production of a variety of derivatives, because of the high reactivity of the strained epoxide ring. For example, monoalcohols, diols, alkoxyalcohols, hydroxyesters, *N*-hydroxyalkylamides, mercaptoalcohols, aminoalcohols, and hydroxynitriles could be produced via epoxide ring-opening reactions with suitable reactants [3].

On an industrial scale, the epoxidation of plant oils is currently carried out with the Prileschajew reaction, in which the unsaturated oils react with a percarboxylic acid, such as peracetic and performic acid, obtained through the acid-catalyzed oxidation of the respective organic acid with hydrogen peroxide [4]. Soluble mineral acids, commonly sulfuric acid, are used as catalysts for this reaction. Therefore, environmental concerns related to the disposal of salts formed during the final neutralization of the mineral acid and technical problems associated with their use, such as corrosion and separation operations, constitute a strong driving force for modification of or the search for a substitute for this technology. The use of heterogeneous catalysts is one of the most attractive possible answers to this challenge [5,6]. For instance, the soluble mineral acid can be replaced by an acid solid [4], or the Prileschajew-type reaction could be replaced by a transition-metal-catalyzed epoxidation.

Ti-containing molecular sieves like Ti–silicalite (TS-1) and Ti-$\beta$ proved to be excellent catalysts for the epoxidation of olefins with aqueous hydrogen peroxide [7] and organic hydroperoxides [8], respectively, but their scope is limited

[*] Corresponding author. Fax: +49 241 8888291.
*E-mail address:* hoelderich@rwth-aachen.de (W.F. Hoelderich).

to small molecules because of the relatively small size of their pores (TS-1, 5.5 Å; Ti-$\beta$, 7.6 × 6.4 Å). Vegetable oils are bulky substrates that do not fit easily into the pores of these materials; for instance, oleic acid methyl ester has a molecular size of ca. 5 × 5 × 5 × 25 Å. Only across its cross section does methyl oleate have access to Ti-$\beta$. To overcome this difficulty, Ti–MCM-41 has been introduced as an effective catalyst for the selective epoxidation of fatty esters with *tert*-butyl hydroperoxide [9]; however, the role of the structure of this catalyst (i.e., hexagonally arranged cylindrical pores of 20–100 Å) has not been discovered. Moreover, the clear advantages of using Ti–MCM-41 catalysts in the epoxidation of this type of substrate, in comparison with the use of amorphous Ti–silicas, have not been discussed.

In this work a comparison of Ti–MCM-41 and Ti–amorphous silicas in the epoxidation of plant oils is reported. Catalytic activity is explained in terms of chemical and textural features of the catalysts, and some other important aspects not previously reported, like temperature and solvent effect, Ti loading, and catalyst re-usability and stability, are also presented.

## 2. Experimental

### 2.1. Catalysts

Ti–MCM-41 materials were prepared according to the procedure developed by Nießen et al. [10], with the use of silica Aerosil (Degussa 200), tetradecyltrimethylammonium bromide (purum; Fluka), tetraethylammonium hydroxide (Fluka; 40 wt% in water), and homemade $(NH_4)_3$ [$TiO_2F_5$] [11]. We produced four Ti–MCM-41 catalysts by changing the amount of Ti source added to the synthesis gel: Ti–MCM-41(0.8), Ti–MCM-41(2.2), Ti–MCM-41(2.7), Ti–MCM-41(2.9). The number in parentheses denotes the molar ratio (Ti/Si) × 100, determined by bulk chemical analysis (ICP-AES).

Four different Ti–amorphous silicas were used: Ti–$SiO_2$(2.0)A is a commercial silica–titania (Grace Davison, type III/2); Ti–$SiO_2$(5.6)B was prepared from coprecipitation of silica Aerosil and tetraethylorthotitanate with tetrapropylammonium hydroxide; Ti–$SiO_2$(0.8)C was prepared in the same way as Ti–MCM-41, but resulted in an amorphous material, according to the XRD and $N_2$ adsorption analysis; and Ti–$SiO_2$(1.6)D was prepared by the same procedure as for the Ti–MCM-41 materials but without the addition of the surfactant. Again, the number in parentheses indicates the molar ratio (Ti/Si) × 100.

### 2.2. Characterization

#### 2.2.1. Catalysts

XRD powder diffraction patterns were collected on a Siemens Diffractometer D5000 equipped with a secondary

monochromator, a variable diaphragm V 20, a nickel filter, and Cu-$K_\alpha$ radiation (wavelength 1.5406 Å); the angle speed was 1.2°/min. Bulk elemental chemical analysis was done by inductively coupled plasma atomic emission spectroscopy (ICP-AES) on a Spectroflame D (Spectro). Typically, 30 mg of sample was dissolved in 500 μl of 40% HF solution, 4 ml of 1:4 $H_2SO_4$ solution, and 45 ml of $H_2O$. FTIR analysis was done on a Nicolet Protégé 460, equipped with a Praying-Mantis unit model HVC-DRP (Harrick) with KBr windows; the spectra were taken at room temperature under a dry air flow. Diffuse reflectance UV/vis spectra were collected on a Lambda 7 (Perkin-Elmer). Samples were not diluted and $BaSO_4$ was used as reference; the recording speed was 60 nm/min, the data interval was 1.0 nm, and the slit width was 4.0 nm. Nitrogen adsorption–desorption isotherms were measured on a Coulter Omnisorp multipoint sorption apparatus; prior to the measurements the samples were degassed for 4 h at 200 °C and $10^{-2}$ Pa.

#### 2.2.2. Reaction mixtures

Reaction mixtures were analyzed by gas chromatography on a Hewlet-Packard HP 6890 with a 60-m FS-SE54 column. Pure products were characterized by GC-mass spectrometry (GC Varian 3400 CX, MS Varian Saturn 3 at 70 eV and electron ionization), infrared spectroscopy (Nicolet Protégé 460, NaCl windows), and $^1$H (300 MHz) and $^{13}$C NMR (75 MHz) in dept90 and dept135 experiments. Hydroperoxide concentration was determined by iodometry.

### 2.3. Catalytic experiments

Epoxidations were carried out in two-necked round-bottomed flasks placed in an oil bath that was kept at the desired temperature. Stirring was done with Teflon-lined magnetic crosses. Oleic acid methyl ester was used as a substrate (Fuchs Petrolub AG, 97 wt% *cis*-9-octadecenoic acid methyl ester). All of the catalysts were evacuated overnight at 120 °C and high vacuum, and kept under argon. Solutions of aqueous *tert*-butyl hydroperoxide in toluene, *n*-hexane, acetonitrile, and *t*-butanol were dried over a molecular sieve (UOP type 3A). Substrate and solvent were mixed for 15 min at the desired temperature, then the catalyst was added, and the mixture was stirred for a further 15 min. Then the hydroperoxide was added at once.

## 3. Results and discussion

### 3.1. Characterization of Ti–MCM-41 catalysts

The hexagonal arrangement of Ti–MCM-41 catalysts was confirmed by the XRD pattern shown in Fig. 1. The peak at ca. 2.2° is due to the diffraction plane 100, which indicates hexagonal symmetry. Two additional high-order peaks were obtained in the case of Ti–MCM-41(2.7) and Ti–MCM-
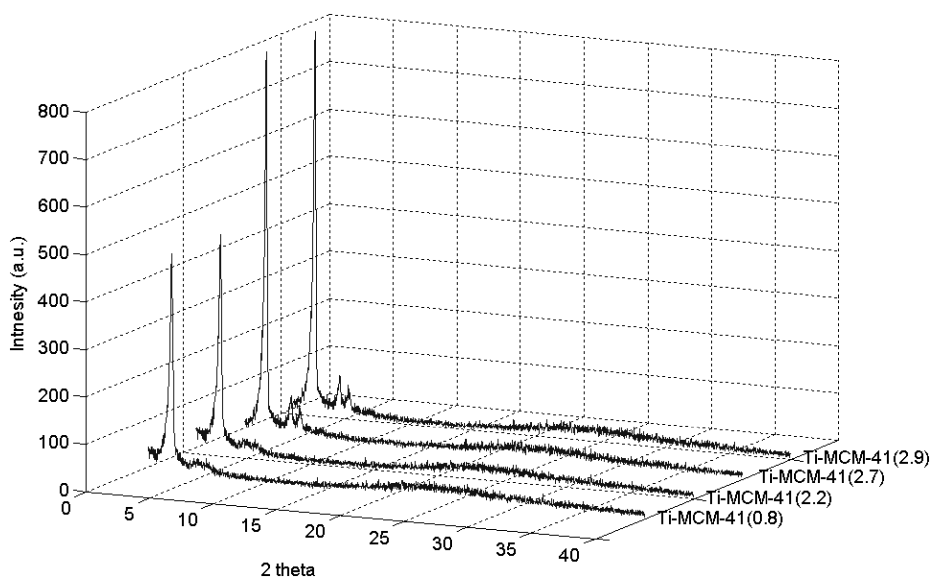
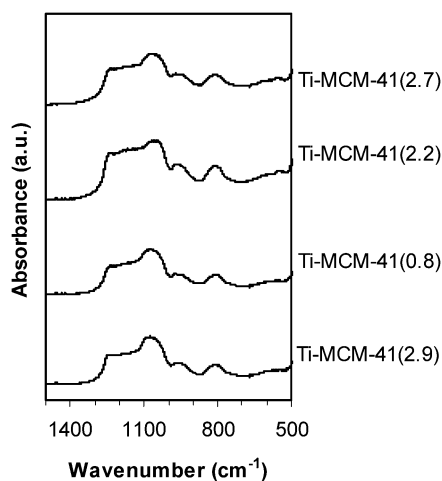Fig. 1. XRD patterns for Ti–MCM-41 catalysts.



Fig. 2. FTIR spectra for Ti–MCM-41 catalysts.



Fig. 3. UV/Vis spectra for Ti–MCM-41 catalysts.

41(2.9); these are related to the diffraction planes 110 and 200.

To evaluate the state of the Ti in the catalyst framework, FTIR and DRS–UV/vis analysis were carried out. The results of these analyses will be discussed in detail because they are crucial to understanding the catalytic behavior that will be displayed later. Results of FTIR measurements are presented in Fig. 2. Four characteristic absorption bands are observed. The band centered at ca. 810 $cm^{-1}$ is due to the symmetric stretching/bending of Si–O–Si bridges. The band at ca. 1085 $cm^{-1}$ with the shoulder at 1220 $cm^{-1}$ arises from the Si–O–Si asymmetric stretching. Finally, the most important band in this context, the band at 960 $cm^{-1}$, is evidence, though not decisive, of the incorporation of Ti into tetrahedral positions in the $SiO_2$ framework. This band is the result of the superimposition of the Si–(OH) stretching mode of the silanol groups with the Si–O–Ti asymmetric stretching mode [12]. The assignation of this band to the Ti site
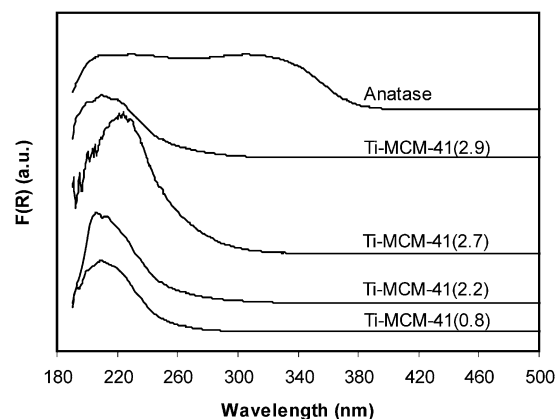
has been the subject of debate; however, there is conclusive support for this assignation [13]. The absence of the band at 960 $cm^{-1}$ would indicate, without any doubt, the non-incorporation of titanium, but its presence is not conclusive enough to prove the incorporation of Ti. Another important issue is that the catalysts do not show absorption bands in the region of 700–400 $cm^{-1}$, which is the range where $TiO_2$ as separated phase absorbs.

The results of UV/vis analysis are presented in Fig. 3. None of the samples show absorption around 340 nm, the wavelength where anatase (shown in the figure) and relatively large $Ti_xO_y$ structures formed by condensed octahedral of Ti absorb [13]. All of the samples have an absorption maximum in the region of 208–220 nm, which is associated with a level-to-level transition due to isolated Ti centers [14]. For example, $Ti[OCH(CH_3)_2]_4$ has an absorption peak centered at 222 nm.

Nitrogen adsorption analysis was carried out to determine some important physical parameters, such as surface area, mesopore volume, and average mesopore diameter. These
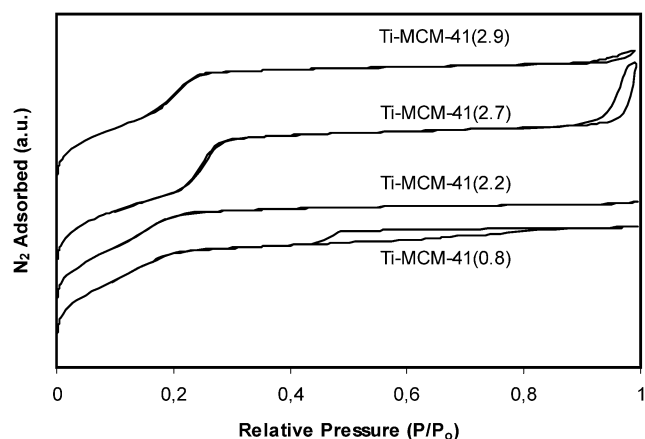
Fig. 4. N$_2$ adsorption isotherms for Ti–MCM-41 catalysts.



$$\varepsilon = V_p \rho / (V_p \rho + 1)$$
$$a_0 = (2/\sqrt{3})(\lambda/(2\sin 2\theta_{100}))$$
$$d_e = a_0 \sqrt{(2\varepsilon(\sqrt{3})/\pi)}$$
$$A_{ext} = A_{tot} - 4V_p/d_e$$
$$h_w = a_0 - d_e$$

Scheme 1. Geometrical model of the hexagonal arrangement of MCM-41 and equations for textural calculations. $\lambda$ = wavelength of X radiation (XRD).



Fig. 5. Effect of temperature on conversion and selectivity during the epoxidation of methyl oleate with Ti–MCM-41(2.7). TBHP/C=C 1.1 mol/mol (amount of C=C calculated from the oil composition measured by GC), oil/catalyst = 20 g/g, toluene/oil = 1 g/g, time = 25 h.

results, together with other analysis like XRD and true solid density, allowed the determination of textural properties that will help to explain the catalytic activity. Fig. 4 shows the nitrogen adsorption isotherms for the Ti–MCM-41 catalysts.

Three of the samples show typical triangle- and parallelogram-shaped hysteresis loops, the latter corresponding to type I (IUPAC). The hysteresis loop is absent in Ti–MCM-41(2.2); this is an indication of a small pore size in this sample [15], a fact that will be confirmed later.
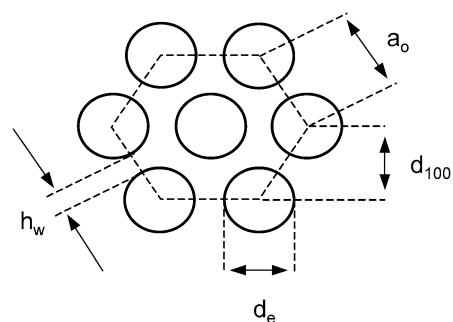
As mentioned before, the textural properties of the Ti–MCM-41 catalysts were determined to establish their influence on the catalytic activity. These properties were calculated by the method proposed by Fenelovov et al. [16]; the results are summarized in Table 1.

The total surface area was calculated with the BET equation, the total pore volume was calculated by the BJH (Barret, Joyner, Halenda) method, true solid density was measured in an auto-pycnometer with helium at 26 °C. The 2$\theta$ angle for the 100 reflection was determined from the XRD pattern; the other parameters were calculated according to the model displayed in Scheme 1.

### 3.2. Catalytic results with Ti–MCM-41

After the characterization of the Ti–MCM-41 catalysts, the activity of these materials on the epoxidation of methyl oleate and its correlation with all of the previous analysis will be discussed. First, the effect of temperature was checked; the results are shown in Fig. 5. An increase in temperature from 25 to 100 °C produces a drop in selectivity of ca. 10%, and the conversion increases from 10 to 90%. The by-product being produced was identified as the ketone obtained from the rearrangement of the epoxidized oil. Although rearrangement of small epoxides is a well-documented reaction [17], to the best of the knowledge of these authors, the rearrangement of epoxidized oils has not yet been reported. Usually the only by-products reported are those from the epoxide ring-opening reactions.

Making a compromise between conversion and selectivity, where the selectivity is ⩾ 95%, results in the selection of
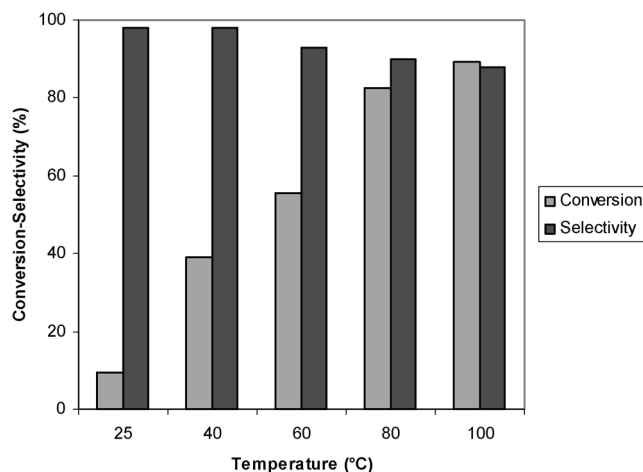
70 °C as the optimal temperature to carry out the reactions comparing the different Ti–MCM-41 catalysts. Fig. 6 shows the results obtained in the epoxidation of methyl oleate catalyzed by the Ti–MCM-41 materials.

The different activities observed were shown to be a function of the level of Ti dispersion (molecular) and textural properties of the supports, such as the external surface area. This latter parameter has not usually been taken into account to explain the activity of mesoporous catalysts, but here it proved to be crucial. Ti–MCM-41(2.7) is the less active catalyst, even though it has a higher Ti loading. This lower activity is a consequence of two factors: (a) Ti is less dispersed than it is in all of the other catalysts because the absorption band in the UV spectra is the most shifted to a higher wavelength, and (b) although the total surface area of Ti–MCM-41(2.7) is comparable to those of Ti–MCM-

Table 1
Textural properties of Ti–MCM-41 catalysts

| Material | Total surface area $A_{tot}$ (m$^2$/g) | Total pore volume $V_p$ (cm$^3$/g) | True solid density $\rho$ (cm$^3$/g) | Internal porosity $\varepsilon$ | $2\theta$ for reflection 100 $2\theta_{100}$ (°) | Util crll parameter $a_0$ (Å) | Pores diameter $d_e$ (Å) | External area $A_{ext}$ (m$^2$/g) | Wall thickness $h_w$ (Å) |
|---|---|---|---|---|---|---|---|---|---|
| Ti–MCM-41(2.7) | 1179 | 1.03 | 2.3 | 0.71 | 2.2 | 46.4 | 41.0 | 169.2 | 5.4 |
| Ti–MCM-41(2.9) | 1354 | 0.72 | 2.5 | 0.64 | 2.8 | 36.4 | 30.5 | 416.2 | 5.9 |
| Ti–MCM-41(0.8) | 1152 | 0.24 | 2.3 | 0.36 | 2.4 | 42.5 | 26.8 | 792.3 | 15.7 |
| Ti–MCM-41(2.2) | 1193 | 0.15 | 2.3 | 0.26 | 2.9 | 35.2 | 18.9 | 870.3 | 16.3 |
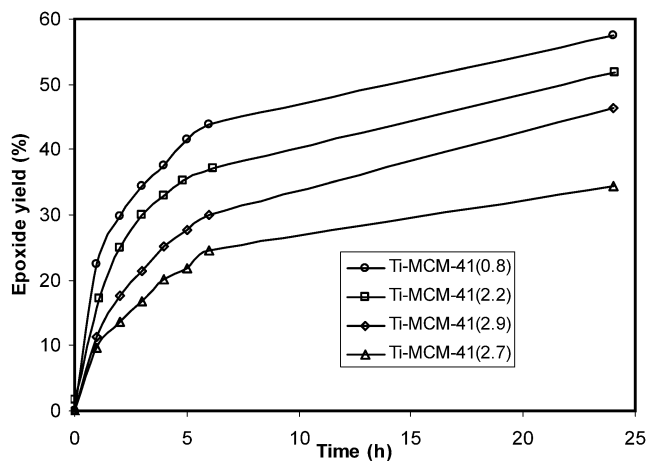


Fig. 6. Comparison of Ti–MCM-41 catalysts for the epoxidation of high oleic methyl oleate. Conditions: TBHP/oleate = 1.1 mol/mol, oleate/catalyst = 20 g/g, toluene/oleate = 1 g/g, temperature = 70 °C.



Fig. 7. UV/Vis spectra for Ti–SiO$_2$ catalysts.

41(0.8) and Ti–MCM-41(2.2), the external surface area is the smallest one (see Table 1).

The relevance of the external surface area for this reaction is confirmed when one compares Ti–MCM-41(2.2) and Ti–MCM-41(2.9). Although the latter has both higher Ti loading, in comparable dispersion degree (based on UV and IR spectra), and a higher total surface area, it is less active. One plausible explanation for this lower activity is the lower external area that Ti–MCM-41(2.9) has compared with Ti–MCM-41(2.2).

The final important issue with regard to Fig. 6 is the superior activity of Ti–MCM-41(0.8). Based on UV and IR spectra and on the very low Ti loading this catalyst has (the lowest one), it can be concluded that it has the highest Ti dispersion. Moreover, this catalyst has a high external surface area comparable to that of Ti–MCM-41(2.2).

One parameter that is of extreme importance for the industrial application of epoxidation technologies is the efficiency in hydroperoxide consumption, which has to be maximized. Table 2 shows the TBHP selectivities for the experiments compared in Fig. 6. Clearly, all of the experiments run with a very high efficiency in the use of the hydroperoxide. This high THBP selectivity results from the relatively fast diffusion of the olefin to the Ti–TBHP peroxo complex, where it takes the oxygen before it is released as gas (peroxide decomposition).
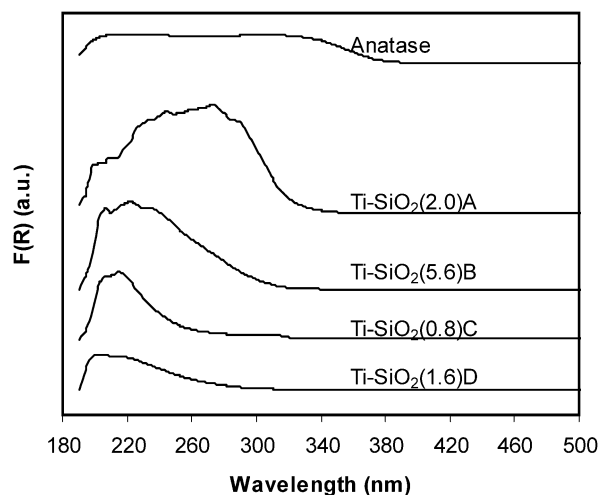
In summary, these results suggest that for the epoxidation of oleic acid methyl ester with TBHP catalyzed by Ti–MCM-41, the two more important catalyst properties are Ti dispersion and external surface area, and both must be high.

After the important conclusion drawn from the epoxidation reactions with Ti–MCM-41 regarding the outstanding role of the external surface area, it was straightforward to reach the idea that a simple amorphous Ti-loaded silica could do also the job, provided the Ti is properly dispersed. Therefore, several Ti/SiO$_2$ catalysts were studied.

### 3.3. Ti–SiO$_2$ catalyst characterization

Fig. 7 shows DRS–UV/vis spectra for the Ti–SiO$_2$ materials. The samples do not show the presence of anatase-like separated TiO$_2$ phase (upper curve). A higher wavelength for the position of the lift-off of the absorption band is linked to a lower Ti dispersion; consequently, the Ti dispersion in these materials follows the order Ti–SiO$_2$(0.8)B > Ti–SiO$_2$(1.6)D > Ti–SiO$_2$(5.6)B > Ti–SiO$_2$(2.0)A, which later will be shown to be in close relation with the activity.

Infrared analyses are presented in Fig. 8. The depression located at ca. 710 cm$^{-1}$ (indicated by the vertical line crossing the figure), which is evidence for the absence of condensed Ti$_x$O$_y$ structures in SiO$_2$(0.8)B, is increasing progressively its intensity in the order SiO$_2$(0.8)B < Ti–SiO$_2$(1.6)D < Ti–SiO$_2$(5.6)B < Ti–SiO$_2$(2.0)A, leading to

Table 2
TBHP selectivity for the experiments of Fig. 6, at 24 h

| Catalyst | 18:1 conversion (%) | Epoxide selectivity (%) | TBHP selectivity[a] (%) |
|---|---|---|---|
| Ti–MCM-41(0.8) | 61.0 | 94.1 | 98.2 |
| Ti–MCM-41(2.2) | 54.5 | 95.2 | 97.3 |
| Ti–MCM-41(2.9) | 49.2 | 94.1 | 99.1 |
| Ti–MCM-41(2.7) | 35.4 | 97.4 | 97.5 |

[a] Selectivity = (mol TBHP reacted with methyl oleate)/(total mol of TBHP consumed). Concentration of TBHP measured by iodometric titration.
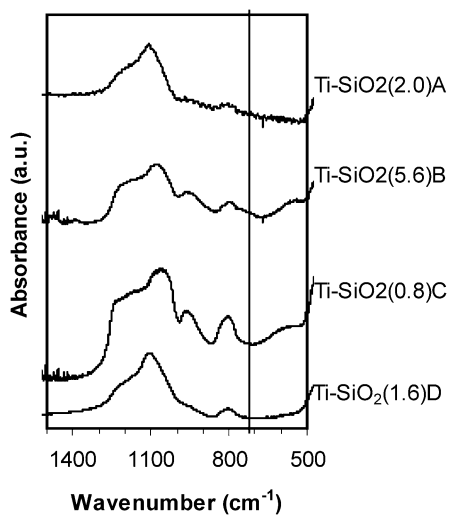


Fig. 8. FTIR spectra for Ti–SiO$_2$ catalysts.



Fig. 9. N$_2$ adsorption isotherms for Ti–SiO$_2$ catalysts.

the same Ti-dispersion order observed in the UV analysis. The band at 960 cm$^{-1}$ appears very weak for the catalyst Ti–SiO$_2$(2.0)A, indicating a low content of framework Ti.

XRD analysis showed that the Ti–SiO$_2$ catalysts are non-crystalline in nature. Nitrogen adsorption isotherms, shown in Fig. 9, were used to calculate the surface area (BET method) and the average pore diameter (BJH method). These two properties are listed in Table 3. Compared with Ti–MCM-41 materials, these Ti–SiO$_2$ catalysts have lower surface areas and larger pore diameters. Later it will be shown (in the discussion of the catalytic results) that this lower surface area is the main factor responsible for the relatively lower activities of some of the Ti–SiO$_2$ catalysts.

### 3.4. Catalytic results with Ti–SiO$_2$

The catalytic results for the epoxidation of methyl oleate with these Ti–SiO$_2$ catalysts are presented in Fig. 10. At 70 °C the selectivity for the desired epoxide is $\geqslant 95\%$.

The activity of these Ti–SiO$_2$ catalysts is in the order Ti–SiO$_2$(0.8)B > Ti–SiO$_2$(1.6)D > Ti–SiO$_2$(2.0)A > Ti–SiO$_2$(5.6)B. This hierarchy is a function of the titanium dispersion and surface area. The average pore diameter does not seem to play an important role in the activity. The most active catalyst, Ti–SiO$_2$(0.8)C, is also the catalyst with the highest surface area (see Table 3) and the catalyst where titanium is more highly dispersed. The latter statement is proved by the lowest Ti content combined with an UV ad-
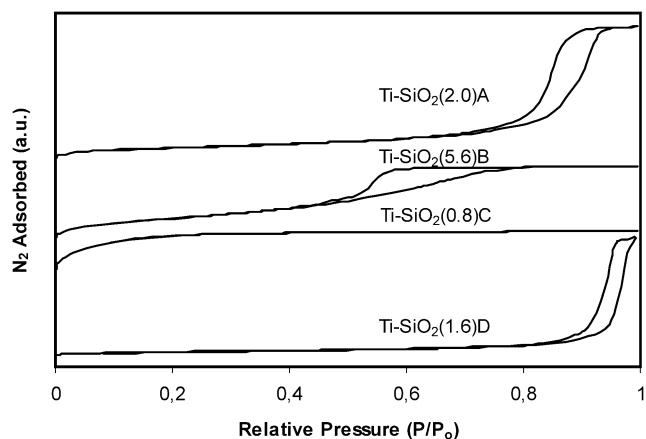
Table 3
Surface area and pore diameter for Ti–SiO$_2$ catalysts

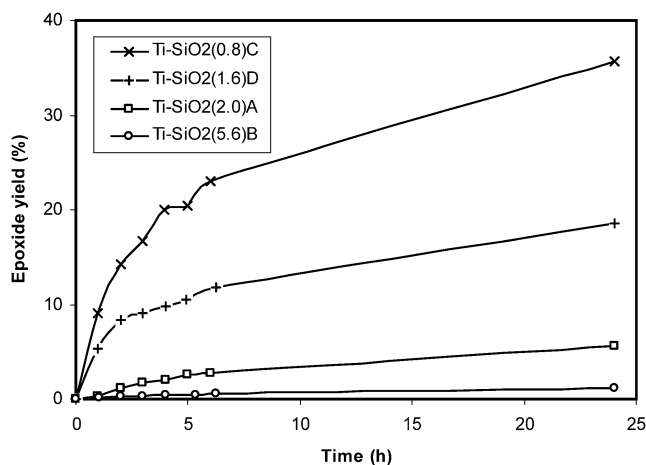| Catalyst | BET surface area (m$^2$/g) | BJH Average pore diameter (Å) |
|---|---|---|
| Ti–SiO$_2$(2.0)A | 310 | 127 |
| Ti–SiO$_2$(5.6)B | 671 | 41 |
| Ti–SiO$_2$(0.8)C | 697 | 29 |
| Ti–SiO$_2$(1.6)D | 124 | 285 |



Fig. 10. Comparison of Ti–SiO$_2$ catalysts for the epoxidation of high oleic methyl oleate. Conditions: TBHP/oleate = 1.1 mol/mol, oleate/catalyst = 20 g/g, toluene/oleate = 1 g/g, temperature = 70 °C.

sorption band shifted to lower wavelength and the less intense 720 cm$^{-1}$ IR band. The second most active catalyst, Ti–SiO$_2$(1.6)D, follows Ti–SiO$_2$(0.8)C in these two factors:
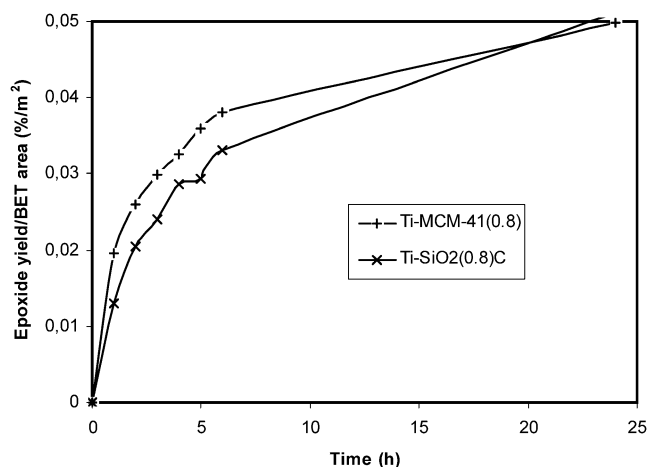
Fig. 11. Comparison of the catalysts Ti–SiO$_2$(0.8) and Ti–MCM-41(0.8) on the epoxidation of high oleic methyl oleate. TBHP/oleate = 1.1 mol/mol, oleate/catalyst = 20 g/g, temperature = 70 °C.



Fig. 12. Solvent effect on the epoxidation of high oleic methyl oleate with Ti–SiO$_2$(1.6)D. hydroperoxide/oleate = 1.1 mol/mol, oleate/catalyst = 20 g/g, toluene/oleate = 1 g/g, temperature = 70 °C.

the UV adsorption band starts at a slightly higher wavelength than on Ti–SiO$_2$(0.8)B, indicating a slightly less Ti dispersion, and it has less surface area. Under the Ti dispersion level of these two catalysts, an increase in Ti loading does not improve the activity.

Although both the Ti dispersion and surface area in Ti–SiO$_2$(5.6)B are higher than in Ti–SiO$_2$(2.0)A, the latter is more active than the former. This behavior can be explained by the fact that the two catalysts are prepared in completely different ways. As mentioned before, Ti–SiO$_2$(5.6)B was prepared by a co-precipitation method, and Ti–SiO$_2$(2.0)A was prepared by impregnation of the already precipitated silica with a titanium salt. This means that part of the Ti in Ti–SiO$_2$(5.6)B could be embedded in the silica matrix, and thus would not b exposed to the surface and, therefore, would be catalytically inactive. In Ti–SiO$_2$(2.0)A all of the Ti must be mainly on the surface, where it is more approachable and thus can more easily react.

Finally, Fig. 11 shows a comparison between Ti–SiO$_2$(0.8)B and Ti–MCM-41(0.8) on the epoxidation oleic methyl oleate; as in the other cases at 70 °C, the selectivity for the epoxide is $\geqslant$ 95%. It is clear that for the epoxidation of high oleic acid methyl ester with TBHP over Ti-containing silicas, it is not necessary to use molecular sieve-based catalysts, which are vitally useful for more demanding reactions that require pore-induced selectivity or a special activation of the active sites provided by the unique electronic and geometrical configuration of molecular sieves. A simple and cheaper silica loaded with titanium is enough to carry out the epoxidation of methyl oleate with TBHP, ensuring that the material has a high surface area and the titanium is finely dispersed.

### 3.5. Solvent effect with Ti–SiO$_2$

All of the previous experiments were carried out with toluene as a solvent; however, it has not been proved that
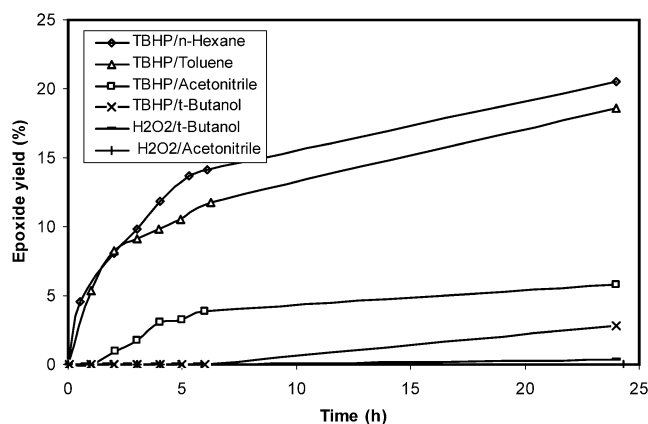
this is the best solvent. The effect of different solvents was evaluated with the catalyst Ti–SiO$_2$(1.6). The results of these experiments are shown in Fig. 12.

The activity for the epoxidation with TBHP increases with the decrease in polarity of the aprotic solvents. The polarity of the aprotic solvents decreases in the order acetonitrile (37.5) > toluene (2.38) > *n*-hexane (1.89) (the number in parentheses is the respective dielectric constant at 25 °C). The activity is diminished by polar protic solvents like *tert*-butanol. However, for the epoxidation with aqueous H$_2$O$_2$, where polar solvents have to be used to avoid a two-phase system, polar protic solvents (*tert*-butanol) perform better than polar aprotic solvents (acetonitrile), although their activity is still too low.

### 3.6. Titanium leaching test on Ti–SiO$_2$

The next step after we made these interesting findings was to evaluate the stability on the Ti–SiO$_2$ catalysts by checking the Ti leaching and the re-usability. These tests were not done on the Ti–MCM-41 materials because their stability and re-usability for this reaction were already reported [8]. The test for titanium leaching was carried out according to the recommendations of Sheldon [18], that is, the catalyst was filtered from the reaction media, at the reaction temperature to avoid re-adsorption of the leached metal or changes on the oxidation state of the metal, and the filtrate was allowed to react further. After removal of the catalyst no further olefin conversion was observed, which can be taken as proof of the absence of Ti leaching, at least during the period of time the catalyst was evaluated. It has been reported before [18,19] that in general Ti-supported catalysts are quite stable toward metal leaching under liquid-phase oxidations, in contrast to V- and Mo-based catalysts, which have shown considerable leaching [20]. It is important to note that the final stability test for catalysts must be done in a bench or pilot plant covering longer reaction times.
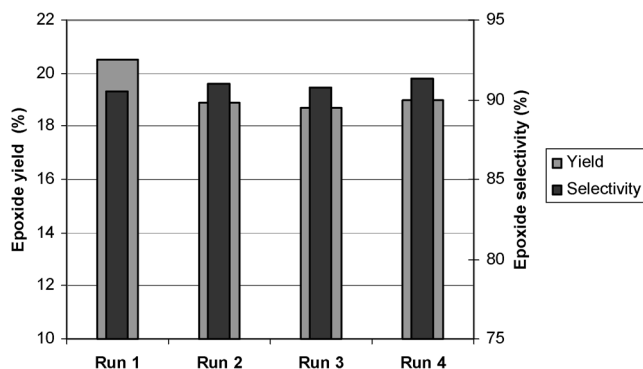
Fig. 13. Leaching test in the epoxidation of high oleic methyl oleate with Ti–SiO$_2$(0.8)C. Conditions: TBHP/oleate = 1.1 mol/mol, oleate/ catalyst = 20 g/g, toluene/oleate = 1 g/g, temperature = 70 °C.

### 3.7. Re-usability of Ti–SiO$_2$

The re-usability of the catalyst was evaluated with four experiments with the same catalyst, which was filtrated after every experiment. Fig. 13 shows that the catalyst is re-usable at least four times, with an initial drop in activity, which can be due to the removal of very fine catalyst particles during the first separation.

## 4. Conclusions

The use of molecular sieves, like MCM-41, as a titanium support, does not offer any additional advantage other than high surface area for the epoxidation of plant oils. The presence of pores is not necessary; the results suggest that the reaction occurs over a large external surface area. The epoxidation can also be carried out with a non-crystalline amorphous Ti–SiO$_2$. The important issue here is to have the titanium center finely dispersed over a relatively high surface area. The temperature should be below 70 °C to minimize ketone formation. The best solvent with this catalyst is one apolar and aprotic, like *n*-hexane. Ti–SiO$_2$ catalyst was shown to be truly heterogeneous under the reaction conditions and was re-usable at least four times. The epoxidation system TBHP/Ti–SiO$_2$ has not been reported so far in the literature for the epoxidation of vegetable oils and methyl oleate, the transesterification product, and, based on the re-sults presented here, it could have a great potential for industrial use.

## References

[1] J.G. Wallace, in: Encyclopedia of Chemical Technology, vol. 9, third ed., Wiley, New York, 1978, p. 263.
[2] U. Biermann, W. Friedt, S. Lang, W. Lühs, G. Machmüller, J.O. Metzger, M.Rüsch gen. Klaas, H.J. Schäfer, M.P. Schneider, Angew. Chem. Int. Ed. 39 (2000) 2209.
[3] H. Baumann, M. Bühler, H. Fochem, F. Hirsinger, H. Zoebelein, J. Falbe, Angew. Chem. 100 (1988) 41.
[4] J. Falbe, in: Methodicum Chimicum, vol. 5, Thieme, Stuttgart, 1975, p. 131.
[5] K. Tanabe, W.F. Hoelderich, Appl. Catal. A 181 (1999) 399.
[6] W.F. Hoelderich, Catal. Today 62 (2000) 115.
[7] B. Notari, Adv. Catal. 41 (1996) 253.
[8] M.A. Camblor, A. Corma, A. Martínez, J. Perez Pariente, J. Chem. Soc. Chem. Commun. (1992) 589.
[9] M.A. Camblor, A. Corma, P. Esteve, A. Martínez, S. Valencia, Chem. Commun. (1997) 795.
[10] T.E.W. Nießen, J. Niederer, T. Gjervan, W.F. Hoelderich, Microporous Mater. 21 (1998) 67.
[11] M.K. Chauhari, B. Das, Inorg. Chem. 25 (1986) 168.
[12] T. Armaroli, Top. Catal. 15 (2001) 63.
[13] M. Rigutto, Vanadium and Titanium-Containing Molecular Sieves, PhD thesis, Technische Universiteit Delft (1996), p. 28.
[14] M.R. Boccuti, K.M. Rao, A. Zecchina, G. Leofanti, G. Petrini, Stud. Surf. Sci. Catal. 48 (1989) 133.
[15] A.V. Neimark, P.I. Ravikovitch, M. Grün, F. Schüth, K. Unger, J. Colloid Interface Sci. 207 (1998) 159.
[16] V.B. Fenelovov, V.N. Romannikov, A.Y. Derevyankin, Micropor. Mesopor. Mater. 28 (1999) 57.
[17] W.F. Hoelderich, in: H. van Bekkum, E.M. Flanigen, J.C. Jansen (Eds.), Introduction to Zeolite Science and Practice, Elsevier, 1991, p. 655.
[18] I.W.C.E. Arends, R.A. Sheldon, Appl. Catal. A 212 (2001) 175.
[19] J.P.M. Niederer, The Preparation of Oxidation Catalysts via a Post-Synthesis Modification of H-[B]-BEA, PhD thesis, University of Technology RWTH-Aachen (2002), p. 100.
[20] J.P.M. Niederer, W.F. Hoelderich, Appl. Catal. A 229 (2002) 51.